Article

Adiabatic Single Scan Two-Dimensional NMR Spectrocopy

Philippe Pelupessy

J. Am. Chem. Soc., **2003**, 125 (40), 12345-12350• DOI: 10.1021/ja034958g • Publication Date (Web): 13 September 2003

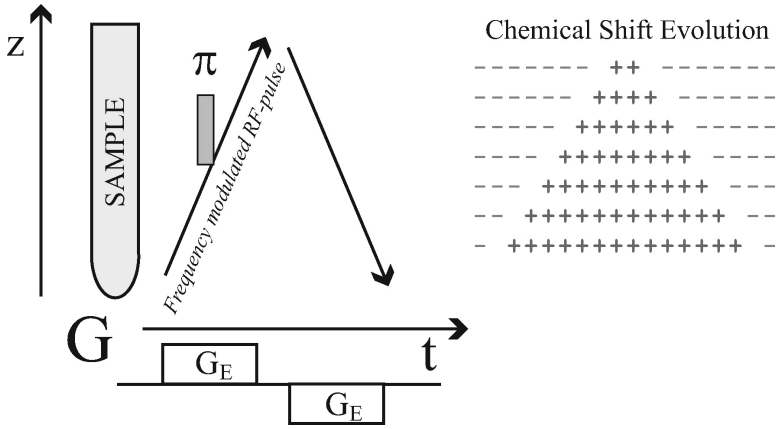

More About This Article

Additional resources and features associated with this article are available within the HTML version:

- Supporting Information
- Links to the 7 articles that cite this article, as of the time of this article download
- Access to high resolution figures
- Links to articles and content related to this article
- Copyright permission to reproduce figures and/or text from this article

View the Full Text HTML

J|A|C|S
ARTICLES
Published on Web 09/13/2003

Adiabatic Single Scan Two-Dimensional NMR Spectrocopy

Philippe Pelupessy*,†

Contribution from the Département de Chimie, associé au CNRS, Ecole Normale Supérieure, 24 rue Lhomond, 75231 Paris Cedex 05, France

Received March 3, 2003; E-mail: philippe.pelupessy@ens.fr.

Abstract: New excitation schemes, based on the use adiabatic pulses, for single scan two-dimensional NMR experiments (Frydman et al., *Proc. Nat. Acad. Sci.* **2002**, *99*, 15 858−15 862) are introduced. The advantages are discussed. Applications in homo- and heteronuclear experiments are presented.

Introduction

The introduction of two-dimensional (2D) experiments has revolutionized the field of nuclear magnetic resonance (NMR).[1,2] Unfortunately, these experiments are inherently time-consuming because many different signals have to be acquired in order to construct a 2D spectrum. Recently, a novel scheme has been presented by Frydman, Scherf, and Lupulescu[3] to record a complete 2D NMR spectrum in a single scan. The principle is achieved by rendering the evolution in one dimension dependent on spatial parameters. The spatial encoding is decoded during detection. This scheme can reduce the time needed to acquire multidimensional NMR experiments by orders of magnitude. We will refer to this type of experiments as Frydman−Scherf−Lupulescu experiments, or FSL experiments.

As an example, we consider a situation where the duration of the chemical shift evolution interval is linearly dependent on the *z*-position of a nucleus. A linear gradient along the *z*-axis suffices to refocus the evolution in this case. The larger the chemical shift, the longer it will take for refocusing to take place. Hence, the echo takes place at a time that will depend on the chemical shift. Frydman et al.[3] achieved the spatial encoding by a train of bipolar gradient pulses combined with frequency-shifted excitation pulses. The spatial encoding is decoded during acquisition by echo planar imaging[4] (EPI). In this article, we propose alternative schemes based on the use of adiabatic pulses to obtain spatially dependent frequency encoding.

Theory

In Figure 1a the original excitation scheme suggested by Frydman et al.[3] is shown. A train of bipolar gradients and, synchronized with the positive gradients, selective excitation pulses is applied. The frequency of the pulses is linearly stepped from the lowest to the highest frequency that is induced by the excitation gradient $\boldsymbol{G}_E$. We assume that a spin $\boldsymbol{S}$ is excited while detection occurs on a spin $\boldsymbol{I}$ after coherence transfer. The phase acquired during the excitation scheme depends on the resonance frequency $\omega_{GE,S}$ induced by the gradient given by $\gamma_S G_E f(r)$ (i.e., $\gamma_S G_E z$ if a linear gradient along the *z*-axis is applied) and the chemical shift $\omega_{CS,S}$ ($= \gamma_S(1 - \sigma_s)B_0$) as

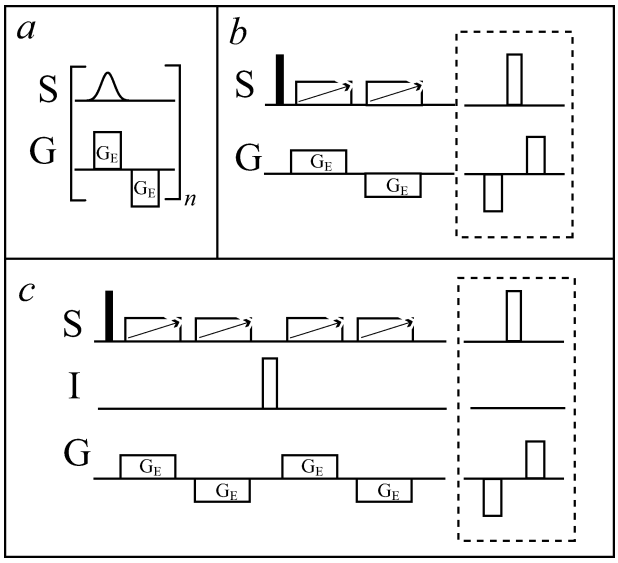

Figure 1. (a) Original excitation scheme proposed by Frydman et al.[3] to obtain the frequency labeling in the indirect ω_1 dimension in Frydman-Scherf-Lupulescu experiments (FSL experiments). A train of bipolar gradients and frequency selective pulses, the carrier frequency of which is stepped from the minimum to the maximum frequency that is induce by the gradients $\boldsymbol{G}_E$, is applied. This causes the evolution time t_1 of the spins $\boldsymbol{S}$ to depend on the sample position. (b) Excitation scheme for modified adiabatic FSL-experiments based on the use of frequency swept pulses during a constant time evolution period. After a nonselective $\pi/2$ pulse, a bipolar gradient pair is applied, while a frequency modulated adiabatic pulse is present during each gradient. In this scheme, the whole sample contributes to the signal and off-resonance effects of the pulses do not deteriorate the excitation profile. Heteronuclear decoupling can be introduced as shown in (c) by repeating the scheme twice, with a π pulse on the **I**-spins in between. The π pulse does not affect the chemical shift evolution of the **S**-spins but inverts the effect of the heteronuclear scalar coupling J_{IS}. The extra blocks in gray can be appended to shift the refocusing of the middle of the chemical shift range of the **S**-spins to the middle of the gradients applied during detection.

† Département de Chimie, associé au CNRS, Ecole Normale Supérieure.

(1) Jeener, J. *Lecture at International Ampère Summer School, Basko, Polje, Yugoslavia*, 1971.
(2) Aue, W. P.; Bartholdi, E.; Ernst R. R. *J. Chem. Phys.* **1976**, *64*, 2229−2246.
(3) Frydman, L.; Scherf, T.; Lupulescu, T. *Proc. Nat. Acad. Sci.* **2002**, *99*, 15858−15863.
(4) Stehling, M. K.; Turner, R.; Mansfield, P. *Science* **1991**, *254*, 43−50.

$$\varphi(G_E,S) = \omega_{CS,S} t_1^{max} \frac{\omega_{GE,S} - \omega_{GE,S}^{max}}{\omega_{GE,S}^{min} - \omega_{GE,S}^{max}} \quad (1)$$

where t_1^{max} is the interval between the first and last excitation pulse. During the detection interval, a gradient $\boldsymbol{G_A}$ with an identical profile as $\boldsymbol{G_E}$ induces a phase

$$\varphi(G_A,I) = \gamma_I G_A f(r) t_A = \omega_{G_A,I} t_A \quad (2)$$

At time $t_A = \tau_R$ the magnetization will have a uniform phase, i.e., form an echo, with

$$\tau_R = \omega_{CS,S} C \quad (3)$$

where C is a constant given by (this constant can be obtained by imposing $d\phi(G_E,S)/dz + d\phi(G_A,I)/dz = 0$)

$$C = \frac{\omega_{GE,S} t_{1,max}}{2\omega_{GA,I}(\omega_{GE,S}^{max} - \omega_{GE,S}^{min})} = \frac{\gamma_S G_E t_{1,max}}{\gamma_I G_A(\omega_{GE,S}^{max} - \omega_{GE,S}^{min})} = \frac{t_{1,max}}{(\omega_{GA,I}^{max} - \omega_{GA,I}^{min})} \quad (4)$$

It has been assumed that G_A and G_E, as well as γ_I and γ_S, have the same sign.

As eq 3 shows, the signal is refocused over the whole sample at a time that is proportional to the chemical shift of spin **S**. The exact shape of the echo will depend on the gradient profile and the sample geometry. During the detection interval, a train of bipolar gradients is applied[3] so that the phase induced by the detection gradients will occur again in a sequence of echoes at $t_A' = t_A + n\tau_A$ and $t_A'' = \tau_A - t_A + n\tau_A$, where τ_A is the duration of the bipolar gradient pair, and n is an integer. Because one bipolar gradient pair must be applied for each t_2 point, the echo must be confined within one-half of the dwell time of the acquisition dimension, i.e., within $1/(2SW_I)$, where SW_I is the spectral width of the **I**-spins. When the full spectral width of the **S**-spins needs to be detected, the maximum evolution time t_1^{max} is therefore limited to

$$t_1^{max} \leq \frac{\nu_{GA,I}^{max} - \nu_{GA,I}^{min}}{2SW_S SW_I} \quad (5)$$

with $\nu_{GA,I}^{max} = \omega_{GA,I}^{max}/2\pi$. The resolution in the indirect dimension depends on the exact profile of the gradients and the sample geometry. Assuming a linear gradient along the z-axis, a cylindrical sample and neglecting relaxation, the signal of the spin **I** during acquisition is given by

$$S(t_A,t_2) = N \int P(S,I) \exp[i\varphi(G_E,S) + i\varphi(G_A,I)] \exp[i\omega_{CS,I}(t_2 + t_A)]dz = P(S,I) \exp[i\omega_{CS,I}(t_2 + t_A)] \exp[i\beta]\mathrm{sinc}[\alpha(t_A - \tau_R)] \quad (6a)$$

for $0 < t_A < 0.5\tau_A$, and

$$S(t_A,t_2) = P(S,I) \exp[i\omega_{CS,I}(t_2 + t_A)] \exp[i\beta]\mathrm{sinc}[\alpha(\tau_A - t_A - \tau_R)] \quad (6b)$$

for $0.5\tau_A < t_A < \tau_A$. N is a normalization factor and $P(S,I)$ is the probability of coherence transfer from spin **S** to spin **I**. The constants α and β are given by

$$\alpha = (\omega_{GA,I}^{max} - \omega_{GA,I}^{min})/2 \quad (7)$$

$$\beta = \omega_{CS,S} t_1^{max}/2 \quad (8)$$

In these equations $0 < t_A < \tau_A$. The signals acquired during each gradient pair are stacked to form the 2D spectrum[3] and t_2 is defined to be zero for all signals stemming from the first slice. The resolution can be defined as the time between the maximum and the first zero-passage of the sinc function

$$\Delta t_A = \pi/\alpha \quad (9)$$

The resolution in the frequency domain of spin **S** is obtained by combining eqs 3 and 9

$$\Delta\nu_{CS,S} = 1/t_1^{max} \quad (10)$$

with $\nu_{CS,S} = \omega_{CS,S}/2\pi$. This scheme suffers from a few drawbacks. First, it is impossible to excite the whole sample, unless one uses pulses with a perfectly square excitation profile. This leads to significant signal losses depending on the excitation profile of the chosen pulse. Off-resonance effects, in particularly Bloch-Siegert shifts,[5] can affect the coherences once they have been excited, leading to deviations in the linearity of the chemical shift evolution as a function of the z-axis. A third source of problems lies in the selectivity of the excitation pulses. The duration of the excitation gradients might be too short to allow a sufficient selective excitation. For example, let us consider a cylindrical sample of 1 cm height and a spectrometer with a proton Lamor frequency of 600 MHz. Let us further assume that the desired resolution requires a $t_1^{max} = 20$ ms and that the excitation uses a train of 20 Gaussian $\pi/2$ pulses using linear bipolar gradients along the z-axis with $G_E = 50$ G/cm. The spread in frequencies induced by the gradients is around 200 kHz for protons. This frequency range needs to be covered by the twenty pulses, hence the frequency steps between consecutive Gaussian pulses can be at most 10 kHz. The selective RF-pulses can have a duration of 500 μs, which leads to an excitation width of about 3 kHz.[6] For protons this does not pose big problems. However, if one wants to excite a nitrogen nucleus with the same excitation scheme, the spread of frequencies created by the gradients is only 20 kHz and the maximum frequency step between the consecutive Gaussian pulses is only 1 kHz.

In Figure 1b, we propose an alternative excitation scheme that does not suffer from the fore-mentioned problems. The scheme starts with a uniform excitation with a nonselective 90° pulse. Hereafter, a gradient is applied, simultaneously with an adiabatic inversion pulse with a linear frequency ramp. After the pulse, the gradient is inverted and an identical adiabatic pulse is applied. The adiabatic pulse covers a frequency range $\Delta\omega_{ad}$ that is larger than the one induced by the gradient. The effect of the first adiabatic pulse is that it will refocus the spins that are near the bottom of the sample first and the ones near the top last, as shown in Figure 2. Although the adiabatic pulse

(5) Emsley, L.; Bodenhausen, G. *Chem. Phys. Lett.* **1990**, *168*, 297−303.
(6) Emsley, L.; Bodenhausen, G. *J. Magn. Reson.* **1989**, *83*, 211−221.

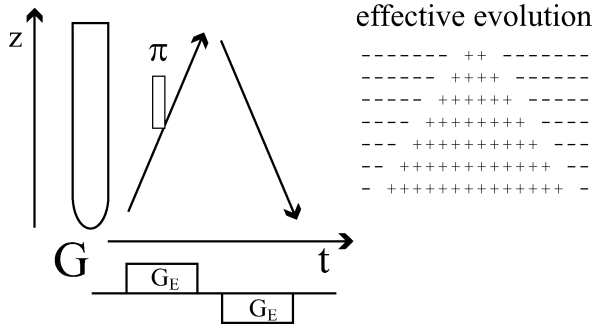

Figure 2. The effect of the two adiabatic pulses in the scheme of Figure 1b can be represented by two instantaneous π pulses that occur when the frequency of the adiabatic sweep passes through the resonance frequency of the spins.[10] Hence the spins near the bottom of the sample are refocused first while the ones at the top are affected last. For the second pulse the situation is time-reversed since the sign of the gradient is inverted. This results in differential evolution throughout the sample, as shown on the right of the figure.

has good inversion properties, it leads to severe phase-distortions when used as a refocusing pulse.[7] The phase at the end of the pulse depends quadratic on the resonance offset.[8−10] To cancel the effect of the offset induced by the gradient, a second adiabatic pulse is applied, but with an inverse gradient. Now, the spins near the top of the sample are refocused first. The overall effect is that the chemical evolution of the spin will be proportional it's *z*-position (see below).

Mathematically, the effect of each adiabatic pulse can be described in terms of two consecutive rotations

$$P_{ad} = \exp(i\pi S_x)\exp(i\varphi S_z) \tag{11}$$

that is, a rotation of 180° around the *x*-axis, followed by a phase-shift ϕ, which depends on the offset with respect to the central frequency of the adiabatic pulse as[8−10]

$$\varphi = \omega_{tot}{}^2\tau_{ad}/\Delta\omega_{ad} \tag{12}$$

with $\omega_{tot} = \omega_{CS,S} + \omega_{GE,S}$ and where τ_{ad} is the duration of the adiabatic pulse. The effect of the two consecutive pulses is

$$P_{tot} = \exp(i\pi S_x)\exp[(i\tau_{ad}(\omega_{CS,S} + \omega_{GE,S})^2/\Delta\omega_{ad})S_z]\exp(i\pi S_x)\exp[(i\tau_{ad}(\omega_{CS,S} - \omega_{GE,S})^2/\Delta\omega_{ad})S_z] \tag{13}$$

which can be written as

$$P_{tot} = \exp[(-i\tau_{ad}(\omega_{CS,S} + \omega_{GE,S})^2/\Delta\omega_{ad})S_z]\exp[(i\tau_{ad}(\omega_{CS,S} - \omega_{GE,S})^2/\Delta\omega_{ad})S_z] = \exp[(-i4\tau_{ad}\omega_{CS,S}\omega_{GE,S}/\Delta\omega_{ad})S_z] \tag{14}$$

This propagator has the desired form. When comparing eqs 1 and 14, one can see that the phase-factors have the same form. The frequency range of each adiabatic pulse has taken the role of the frequency range of the gradient $\boldsymbol{G}_E$. Because the frequency range of the adiabatic pulse has to be larger than the one induced by the gradient, the effective t_1 evolution time is reduced. On the other hand, the term $4\tau_{ad}$ replaces t_1^{max}. $4\tau_{ad}$ is twice the duration of the adiabatic pulses. The constant time is thus used twice as efficiently as the time in the real time experiments. This is due to the fact that the effective chemical shift evolution can take place between $-2\tau_{ad}$ and $+2\tau_{ad}$. In a normal constant time experiment, this can also be achieved in principle by defining the first t_1 point with a π-pulse on the left of a constant time interval and moving the RF pulse to the right. However, a very large first-order phase correction would be needed to correct the phases in the resulting spectrum. Therefore, one usually starts with the π-pulse in the middle of the constant time period.[11] In eq 1, there is also an additional term which does not depend on $\omega_{GE,S}$. This term is responsible for the phase-factor β in eq 6. With the adiabatic scheme this phase-factor will be zero (if $\omega_{GA,I}^{max} = -\omega_{GA,I}^{min}$). The choice of the adiabatic pulse shape is not very important as long as it leads to a quadratic dependence of the phase shift with respect to the offset. In this work, we have only looked at systems for which relaxation was not important. We chose a smoothed chirp[12] with a generous frequency-range as a pulse. Simulations showed it had a suitable offset dependence over the frequency range induced by the gradient $\boldsymbol{G}_E$. When transverse relaxation is important, one should chose an adiabatic pulse with a range that is as close as possible to the frequency range that is induced by the gradient while keeping an ideal quadratic phase profile. We are currently investigating which pulses are best used in situations with rapid transverse relaxation.

As shown in Figure 1b, in order to have the spins with zero chemical shift (i.e., on resonance with respect to the central frequency of the chirps) appear in the middle of the detection gradients $\boldsymbol{G}_A$, an echo with a bipolar gradient can be applied with gradients that must be equal in strength (multiplied by the ratio γ_I/γ_S) and of one-quarter of the duration as the gradients used in the detection block. The same effect can be achieved by setting the central frequency of the adiabatic pulses near the edge of the chemical shift range.

There are several advantages of this adiabatic scheme: (a) the whole sample contributes to the signal; (b) there are no problems due to Bloch-Siegert effects; and (c) no strong gradients are needed in the encoding phase (as in the original FSL experiments there is still a need for strong gradients during detection). Heteronuclear decoupling can be easy incorporated, as shown in Figure 1c. The disadvantages of the adiabatic scheme are that one suffers more from losses due to T_2 and to evolution under homonuclear scalar couplings. These effects are at least partially compensated by the doubling of the effective t_1 evolution time. Note also that in the original scheme with discrete excitation, chemical shifts which are separated by $\Delta\omega_{CS,S} = 2\pi/\tau_E$, where τ_E is the interval between two consecutive excitation pulses, are indistinguishable, so that the spectral width SW_S in the indirect dimension is limited. In the detection part, the same spectral width is also limited by the strength and the duration (i.e., the dwell-time in the direct dimension, see eq 5) of the gradients $\boldsymbol{G}_A$. Peaks that lie outside the chosen spectral width will get folded into the spectrum, provided that the spectral widths SW_S, selected during excitation and detection, are carefully matched. In the adiabatic scheme, peaks that lie outside the chosen spectral width are simply cut off.

(7) Ugurbil, K.; Garwood, M.; Rath, A. R.; Bendall, M. R. *J. Magn. Reson.* **1988**, *78*, 472−497.
(8) Cano, K. E.; Smith, M. A.; Shaka, A. J. *J. Magn. Reson.* **2002**, *155*, 131−139.
(9) Hallenga, K.; Lippens, G. M. *J. Biomol. NMR* **1995**, *5*, 59−66
(10) Zwahlen, C.; Legault, P.; Vincent, S. J. F.; Greenblatt, J.; Konrat, R.; Kay, L. E. *J. Am. Chem. Soc.* ***1997***, *119*, 6711−6721.
(11) Bax, A.; Mehlkopf, A. F.; Smidt, J. *J. Magn. Reson.* **1979**, *35*, 373−377.
(12) Böhlen, J. M.; Bodenhausen, G. *J. Magn. Reson. A* **1992**, *102*, 293−301.

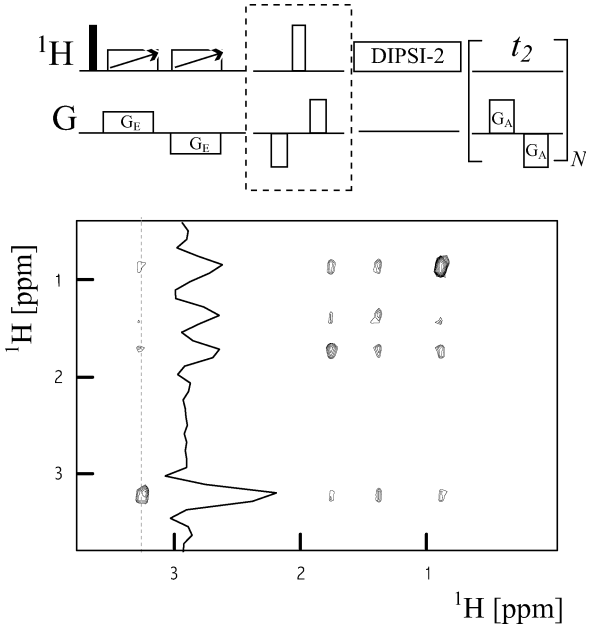

Figure 3. Scheme of Figure 1b followed by a TOCSY mixing sequence and the EPI-detection block. The experiment has been applied to a sample of 10% (vol/vol) *n*-butylbromide in $CDCl_3$.

Translational diffusion will affect both schemes. The effect of frequency labeling is identical to a gradient applied on spin **I** with a duration τ_R and a strength G_A. The phase dispersion due to this gradient is refocused during detection. The diffusion losses will thus depend on the interval between excitation and detection, which increases with increasing t_2. Note that the diffusion losses depend on the chemical shifts of the **S**-spins, which are proportional to τ_R. In particular, when the mixing sequences are long (as in NOESY-experiments) and the molecules are small, the losses can be considerable. The adiabatic scheme might be slightly more prone to diffusion losses *during* excitation than the original discrete scheme, because longer bipolar gradients are applied, although these gradients may be weaker and the total t_1 evolution shorter.

Results

To test the adiabatic scheme, it has been combined with a TOCSY[13] mixing sequence and the EPI detection scheme as in the original FSL-experiments[3] (we will refer to this experiment as FSL-TOCSY). In Figure 3, the results can be seen for a sample of 10% (vol/vol) *n*-butylbromide of in $CDCl_3$. A vertical cross-section through one of the peaks is also presented, showing the sinc profiles of the signals. This might cause problems, particularly when signals with a large dynamic range of amplitudes appear close together. To reduce the "truncation" artifacts, several strategies are possible. The first option might lie in improved signal processing, for example an inverse Fourier transform, followed by a multiplication with a window function before returning to the frequency domain. The second option is to improve the pulse design, in such a way that the excitation profile is not square, for example by deliberately violating the adiabatic condition at the edges of the sample. Other solutions might lie in changing the sample geometry or the gradient profile. These latter options seem particularly attractive when the quantity of the solute (rather than its concentration) is limited. Note that the resolution in the ω_2 dimension is also a limited. In fact, just 32 complex points are recorded in the t_2 domain. Hence, a total of 64 gradients of 200 μs duration each where applied during detection. These gradients had a strength of 25 G/cm (i.e., 50% of the maximum strength). Even if the probe may be sturdy enough to allow the application of gradients during a considerable longer duration, it appears prudent to stay well within the limits of the probe. As eqs 5 and 10 show, large gradients need to be applied when large spectral widths need to be covered in both dimensions and when high resolution needs to be obtained in the indirect ω_1 dimension. This might not be a problem when acquiring a single-scan two-dimensional experiment, since the recovery-delay is infinite. However, when incorporating the FSL scheme into higher-dimensional experiments heating of the probe might become a problem. Note that the use of mixing sequences that transfer both *x*- and *y*-components of the coherences[14] leads to a 2-fold gain in the signal-to-noise ratio in FSL experiments.

We incorporated the scheme of Figure 1c into an FSL-HSQC.[15] In the sequence shown in Figure 4a, a few precautions were taken to suppress signals from protons that are bound to ^{12}C. First a strong purging gradient is applied after the conversion from H_z into $2H_zC_z$ and a $\pi/2$ pulse is inserted after the last INEPT sequence. Moreover, in the last block of the sequence of Figure 1c we increased the gradient strength, the effect of which is refocused with an additional echo just before acquisition. For fast relaxing nuclei, it might be better to remove the last $\pi/2$ pulse and refocusing the effect of the increased gradient strength in the excitation scheme within the last INEPT step. Figure 4b and 4c show the results of the sequence applied to the same sample with ^{13}C in natural abundance as in Figure 3. In Figure 4b, no carbon decoupling is applied. The fact that strong gradients are applied during detection decreases the decoupling efficiency because the carbon resonances are spread over a wide frequency range. This deteriorating effect seems to be compensated partially by the fact that the off-sets are switched from positive to negative. In Figure 4c, GARP decoupling[16] with an RF strength of 3 kHz has been applied. Indeed, the peak height of the proton singlet is lower than the sum of the peak heights of the coupled multiplet, as can be seen from the traces in Figure 4d. Tailored decoupling sequences will need to be designed to obtain optimum signal intensities (we tried several known decoupling sequences, but were not able to improve on this result). The sample concentration was about 1 M, thus the peak heights correspond to concentrations of about 10 mM.

In Figure 5(top) the same sequence is applied to a sample of ^{13}C-labeled glucose in D_2O. Care has been taken to have the constant time period (the duration of the four adiabatic pulses plus the additional block) around $1/J_{CC}$. The selected spectral width in the proton ω_2 dimension does deliberately exclude the anomeric proton. However, protons that lie outside this region will in principle appear folded into the spectrum. But, since the anomeric carbon frequency lies outside the chosen spectral width in the carbon ω_1 dimension, as shown in the traditional HSQC spectrum of Figure 5 (bottom), the resonance is eliminated from the spectrum.

(13) Braunschweiler, L.; Ernst, R. R. *J. Magn. Reson.* **1983**, *53*, 521−528.
(14) Shaka, A. J.; Lee, C. J.; Pines, A. *J. Magn. Reson.* **1988**, *77*, 274−293.
(15) Bodenhausen, G.; Ruben, D. J. *Chem. Phys. Leyt.* **1980**, *69*, 185−189
(16) Shaka, A. J.; Barker, P. B.; Freeman, R. *J. Magn. Reson.* **1985**, *64*, 547−552.

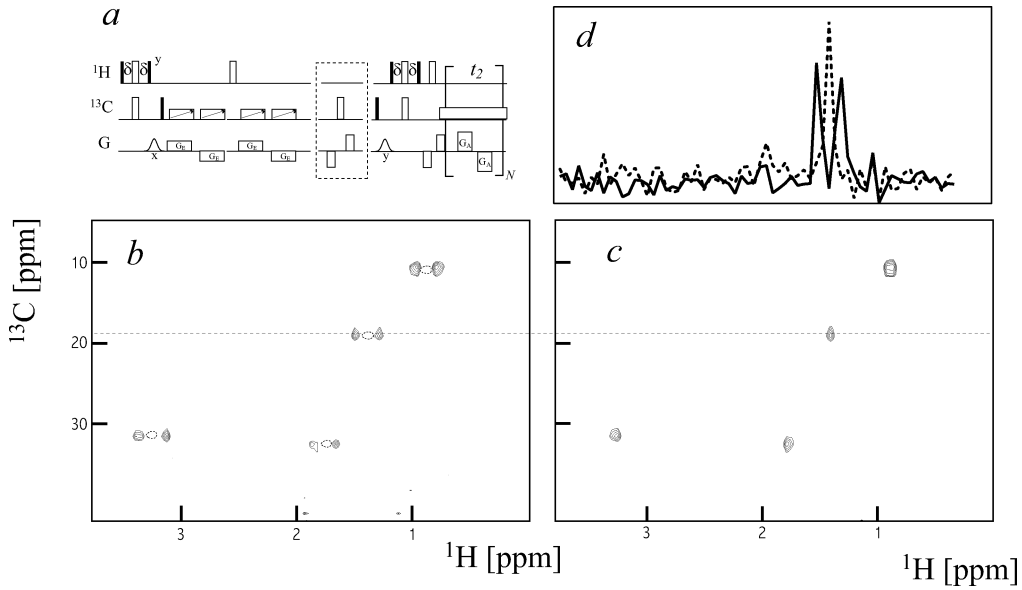

Figure 4. (a) Scheme of Figure 1c incorporated into an FSL-HSQC. All RF-pulses are applied along the *x*-axis and gradient pulses along the *z*-axis, unless indicated otherwise. The delay $\delta = 1/4^1J_{CH}$. The experiment has been applied to a sample of *n*-butylbromide of 10% (vol/vol) in $CDCl_3$ with ^{13}C in natural abundance. (b) Coupled spectrum (the dotted circles show the peaks in a traditional HSQC-experiment). (c) Carbon-decoupled spectrum. (d) Horizontal cross-sections through (b) and (c).

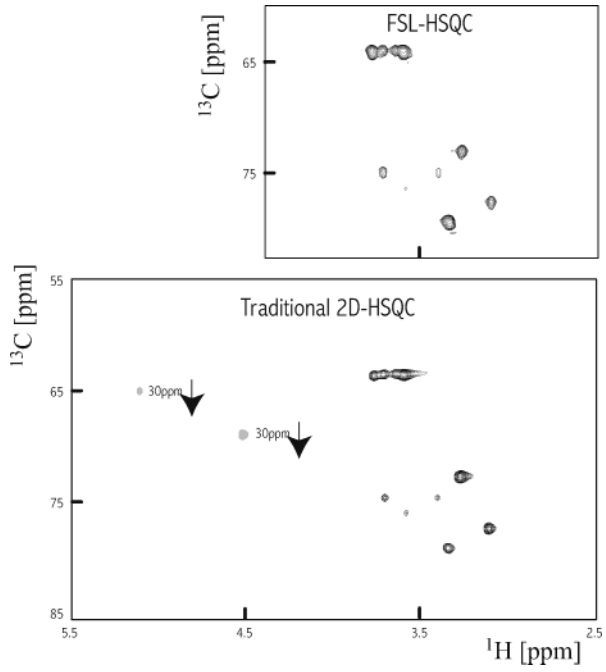

Figure 5. (top) Experiment of Figure 4c applied to a sample of ^{13}C labeled glucose in D_2O. (bottom) Traditional HSQC applied to the same sample. The cross-peaks that belong to the anomeric protons present in the traditional HSQC do not appear in the FSL-HSQC, because the anomeric carbon frequencies lie outside the chosen spectral width of the ω_1 dimension.

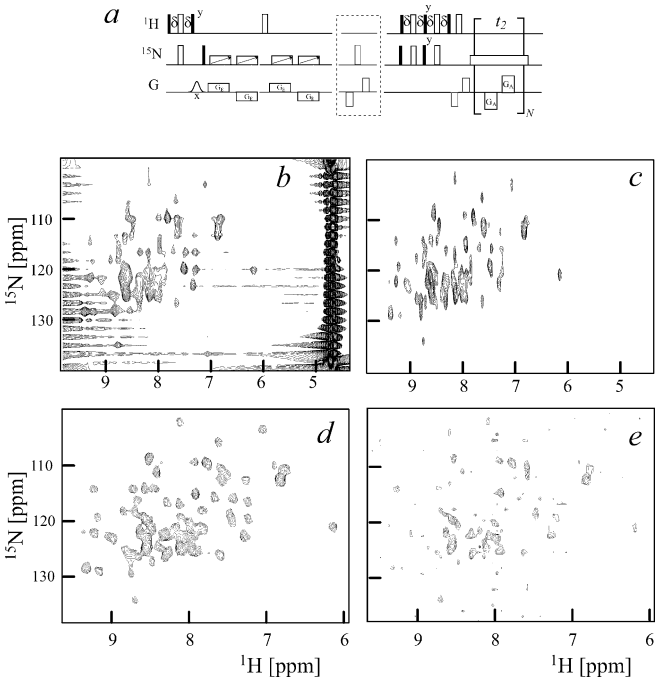

Figure 6. (a) Scheme of Figure 1c incorporated into a sensitivity-enhanced HSQC-experiment. All RF-pulses are applied along the *x*-axis and gradient pulses along the *z*-axis, unless indicated otherwise. The delay $\delta = 1/4^1J_{NH}$. (b) Experiment applied to a sample of ^{15}N labeled human ubiquitin. The experiment has been repeated with 128 identical scans to enhance signal-to-noise ratio. (c) Same as (b) but the phase of the first nitrogen $\pi/2$ pulse has been alternated between consecutive experiments in order to suppress the residual water signal. (d) Same as (c) but the proton carrier frequency is shifted to the middle of the amide proton range and a smaller spectral width is chosen. (e) Same as (d) but only two scans have been recorded with phase alternation.

The FSL sequences are particularly interesting in situations where fast acquisition is crucial. For proteins it could be used to acquire a full *N*-dimensional spectrum in the time that it usually requires to acquire an *N-1*-dimensional spectrum[3]. It could also be applied to protein folding studies. We have introduced our scheme into a sensitivity-enhanced HSQC experiment[17] and applied the sequence to a sample of ^{15}N labeled human ubiquitin (1 mM, 300μL). In Figure 6b the resulting spectrum is shown. For this spectrum, 128 identical scans have been averaged. The first thing to notice is the poor quality of the water suppression, even if strong gradients were applied. The water signal is a nuisance, particularly because it gets folded into the left part of the spectrum. One could increase the spectral

(17) Kay, L. E.; Keifer, P.; Saarinen, T. *J. Am. Chem. Soc.* **1992**, *114*, 10 663−10 665.

width in the proton dimension but then the resolution in the nitrogen dimension would suffer (see eqs 5 and 10). Clearly, better suppression schemes are needed in order to obtain a single-scan two-dimensional spectra in a protonated solvent. We were able to suppress the water signal completely by phase alternating the first nitrogen $\pi/2$ pulse (Figure 6c). Having suppressed the water signal, the spectral width in the proton dimension could be reduced to cover just the amide region (Figure 6d). For the spectrum of Figure 6d, 128 phase-alternated scans have been acquired. The quality of the spectrum shows that the technique is applicable to higher dimensional experiments, where it is often not the signal-to-noise ratio but the need to have sufficient resolution that dictates the experimental duration. In the Supporting Information the spectrum of Figure 6d is compared to a traditional sensitivity-enhanced HSQC. The sensitivity of FSL experiment decreases due to the fact that the dwell-time in the direct dimension needs to be shorter[3] so that more noise is collected. The noise increases by $\sqrt{2n}$, where n is the amount of points that is acquired per gradient during the detection. Due to the fact that the signals acquired during the positive and negative gradients are summed the final signal-to-noise ratio will decrease by $\sqrt{n}$. The minimum amount of points that needs to be acquired per detection gradient is

$$n_{\min} = \tau_A/2\Delta t_A \tag{15}$$

where Δt_A is the resolution as defined in eq 9. This minimum amount of points determines the optimum sensitivity the can be obtained in FSL experiments (note that when less points are acquired one risks to leave some peaks undetected). Above comparison is valid when the two experiments are acquired with the same amount of scans. When the signal is obtained in a single scan the signal-to-noise decreases with another factor $\sqrt{ns}$, with ns the total amount of scans that needs to be acquired with the traditional 2D-experiment. It is clear that when time is not an issue the traditional approach is preferable. The one-scan experiment has as an advantage that the full polarization is detected, since no recycle delay is needed.

In Figure 6e, we have the same experimental conditions as in Figure 6d except that only two scans have been applied. Note that with the currently available technology, i.e., cryogenic probes and/or higher magnetic fields, a considerable gain in sensitivity could be achieved. With a gain of a factor eight in signal-to-noise the spectrum of Figure 6d could be acquired in two scans with alternating phases.

Experimental Section

The experiments were acquired with a Bruker Avance-600 MHz spectrometer equipped with a triple resonance TBI probe with triple axis gradients. All experiments were single scan acquisitions except the experiments in Figure 6. The experiments in Figures 3 and 4 were performed on a sample of unlabeled *n*-butylbromide in $CDCl_3$ at 22 °C, the experiments in Figure 5 on a mixture of ^{13}C labeled $\alpha(+)$- and $\beta(+)$-glucose in D_2O at 22 °C and the experiments in Figure 6 on ^{15}N labeled human ubiquitin in H_2O at 30 °C. For the FSL-TOCSY in Figure 3, the following experimental parameters were used: 32 bipolar gradient pairs during detection with rectangular gradients $\boldsymbol{G}_A$ of 200 μs duration and 25 G/cm strength each; one bipolar excitation gradient pair with gradients $\boldsymbol{G}_E$ of 5 ms and 3.5 G/cm each; the adiabatic pulse had a length τ_{ad} of 5 ms and a sweep range $\Delta\nu_{ad}$ of 30 kHz. For the FSL-HSQC in Figure 4: 32 detection gradient pairs, with $\boldsymbol{G}_A$ of 200 μs and 25 G/cm; $\boldsymbol{G}_E$ of 2.5 ms and 4 G/cm; $\tau_{ad} = 2.5$ ms, $\Delta\nu_{ad} = 25$ kHz. For the FSL-HSQC of Figure 5: 64 detection gradient pairs, with $\boldsymbol{G}_A$ of 400 μs and 12.5 G/cm; $\boldsymbol{G}_E$ of 5 ms and 4.5 G/cm; $\tau_{ad} = 5$ ms, $\Delta\nu_{ad} = 30$ kHz. For the sensitivity enhanced FSL-HSQC in Figure 6b and 6c: 64 detection gradient pairs, with $\boldsymbol{G}_A$ of 120 μs and 25 G/cm; $\boldsymbol{G}_E$ of 5 ms and 3.5 G/cm; $\tau_{ad} = 5$ ms, $\Delta\nu_{ad} = 10$ kHz. For the sensitivity enhanced FSL-HSQC in Figure 6d and 6e: 32 detection gradient pairs, with $\boldsymbol{G}_A$ of 200 μs and 25 G/cm; $\boldsymbol{G}_E$ of 5 ms and 6 G/cm; $\tau_{ad} = 5$ ms, $\Delta\nu_{ad} = 10$ kHz. The spectra where processed using home-written routines in Scilab.[18] The spectra were zero-filled once and Fourier transformed in the direct ω_2 dimension. A first-order phase-correction was applied according to eq 6 (with $\beta = 0$). No window functions have been applied, except for the spectrum in Figure 6b, where the t_2 dimension has been apodized by a cosine-bell window.

Conclusions

In this paper, we have introduced an adiabatic scheme to improve experiments, invented recently by Frydman et al.[3], that allow one to acquire 2D spectra in one scan. The scheme uses frequency modulated adiabatic chirp pulses to obtain a spatially dependent frequency labeling. There are several advantages of the new scheme: the whole sample contributes to the signal, off-resonance effects are eliminated, the constant time evolution can be used almost twice as efficiently and no strong gradients are needed in the excitation phase. With respect to the original FSL experiments, the new scheme is particularly attractive for heteronuclear experiments and low sample concentrations.

Acknowledgment. We thank Dr. Geoffrey Bodenhausen and Dr. Teresa Damiano for useful comments on the manuscript. This work was supported by the European Union through the Research Training Network "Cross-Correlation" HPRN-CT-2000-00092 and by the Centre National pour la Recherche Scientifique (CNRS) of France.

Supporting Information Available: A traditional SE-HSQC spectrum taken under the same conditions as the spectrum in Figure 6d. This material is available free of charge via the Internet at http://pubs.acs.org.

JA034958G

(18) Software package for numerical computations, freely available at http://www-rocq.inria.fr/scilab/.